Transient D″ discontinuity revealed by seismic migration

K. Chambers[1] and J. H. Woodhouse[1]

Received 30 May 2006; revised 25 July 2006; accepted 1 August 2006; published 9 September 2006.

[1] The D″ region beneath North Central Asia is investigated using a weighted migration based on the Generalised Radon Transform. We image complex structure including a D″ discontinuity with variable topography and velocity contrast. We also present observations of an area where the D″ reflector stops. Using synthetic data sets generated for distributions of point scatterers we show that this is not due to deficiencies in the data coverage, but requires that the D″ discontinuity is not a continuous surface. The termination of the discontinuity appears to restrict it to a region high seismic velocity. This could be interpreted as confirmatory evidence for the existence and behaviour of the post-perovskite phase transformation. However, compositional variations may also play a role.
Citation: Chambers, K., and J. H. Woodhouse (2006), Transient D″ discontinuity revealed by seismic migration, *Geophys. Res. Lett.*, *33*, L17312, doi:10.1029/2006GL027043.

1. Introduction

[2] Despite the region's importance for understanding processes such as mantle convection and mixing, the distribution of chemical heterogeneity in the mantle and core-mantle coupling, the bottom 200–400 km of the mantle (also referred to as D″ region or the lowermost mantle) remains poorly understood. A particularly enigmatic feature of this region is the intermittent presence of the D″ discontinuity, which marks the upper surface of the D″ region in some areas. Possible causes for the D″ discontinuity include thermal or compositional gradients. Although recent results from mineral physics have also suggested a phase change in perovskite as candidate mechanism [*Murakami et al.*, 2004].

[3] Despite observations in many regions with a variety of different data types the D″ discontinuity has not been established as a global surface because of several areas where no discontinuity is observed [*Wysession et al.*, 1998]. Failure to observe the D″ reflector could be attributed either to topography and focusing effects related to a continuous global surface; alternatively the discontinuity may be a transient feature which is absent in some regions and present in others.

[4] Recent seismological studies of structure in the D″ region have either concentrated on the use of un-weighted migrations to analyse the structure in specific regions [*Bilek and Lay*, 1998; *Kito and Kruger*, 2001; *Thomas et al.*, 2004b, 2004a] or have used global travel time data sets to constrain the very long wavelength structure via seismic tomography [*Liu and Dziewonski*, 1998; *Castle et al.*, 2000]. In this study we investigate the lowermost mantle beneath Siberia. This area has been the subject of several previous studies [*Gaherty and Lay*, 1992; *Houard and Nataf*, 1993; *Kendall and Shearer*, 1994; *Bilek and Lay*, 1998; *Thomas et al.*, 2002, 2004b] and D″ structure in this region is typically modeled using a 2.75% increase in S-wave velocity 290–320 km above the core-mantle boundary (CMB) [*Lay and Helmberger*, 1983; *Gaherty and Lay*, 1992]. Although recent studies have also shown that the depth of the D″ discontinuity varies by up to 100 km [*Thomas et al.*, 2004b; *Hutko et al.*, 2006] in this and other regions. In addition to arrivals from the D″ reflector other phases have been associated with reflectors ~130 km above the CMB [*Bilek and Lay*, 1998], and velocity decreases 50–80 km above the CMB [*Thomas et al.*, 2004b].

[5] Here we apply a seismic migration/inversion technique to a data set of long-period waveforms in order to image structure in the D″ region. In an earlier publication [*Chambers and Woodhouse*, 2006] we developed the method and studied the D″ region beneath Alaska. Here we extend the results to the lowermost mantle beneath Siberia. We present observations of an area where the D″ reflector varies in velocity contrast and stops. By migrating synthetic data sets made using distributions of point scatterers we test the resolution of our results. The tests show that variation of the velocity anomaly of the D″ discontinuity is not due insufficient sampling of the region or wave propagation effects related to topography of a continuous surface.

2. Method

[6] The details of our data processing and modeling technique are already presented by *Chambers and Woodhouse* [2006], so here we limit discussion to a brief summary of the approaches used. Our working data set consists of ~500 transverse component records that are sensitive to structure in the North Central Asia region. The data are for epicentral distances in the range 60–75 degrees, filtered between 15 and 75 seconds. The low frequency nature of the data and the epicentral distance range means that signals from the lower mantle are obscured by the larger *S* and *ScS* phases. In order to retrieve these signals we apply a phase stripping technique [*Kendall and Shearer*, 1994]. A reference pulse is made for each trace using the scaled first half of the *S* pulse and the second half of the *ScS* phase. By aligning the pulse with the *S* and *ScS* phases and subtracting this signal from the data a phase stripped trace is made, this contains scattered arrivals from the lower mantle. Examples of waveforms as well as further discussion of the phase stripping procedure are available as auxiliary material[1].

[7] The phase stripped traces were converted to zero phase by subtracting the phase spectra from the reference

[1]Department of Earth Sciences, University of Oxford, Oxford, UK.

0094-8276/06/2006GL027043

[1]Auxiliary materials are available in the HTML. doi:10.1029/2006GL027043.

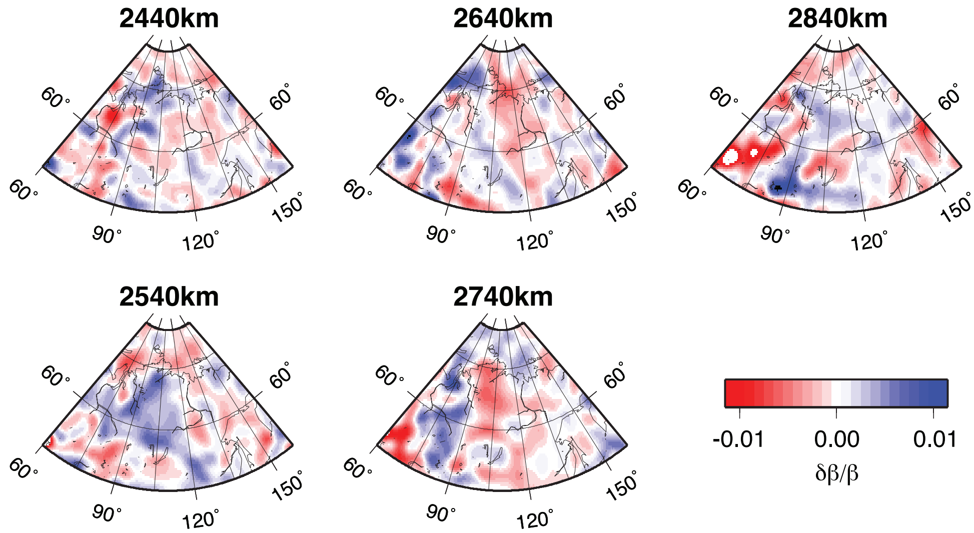

Figure 1. Map sections through the migration results. The migration retrieves discrete jumps in S-wave velocity ($\delta\beta/\beta$). The major structure is at 2540 km depth. Velocity anomalies are also retrieved in the southwest at 2740 km and in the bottom 100 km of the mantle in the regions centre. Smaller features could be artifacts of noise in the data and a biased experimental geometry. The very low amplitudes in the south-western corner at 2840 km depth are in region of poor sampling (see Figure 2e) and so is unlikely to be genuine structure.

pulse, and used as the data for a weighted migration based on the inverse scattering approach of *Miller et al.* [1987] (the Generalised Radon Transform, GRT). The process can be summarised as a diffraction stack migration which uses weights to compensate for the affects of source and scatterer radiation patterns as well as geometrical spreading, in order to retrieve S-wave velocity perturbation from an unperturbed background model. The migration space consists of image points placed at 50 km intervals in the lowermost 800 km of the mantle. For each image point we select amplitudes appropriate to the predicted travel time for the source-image point-receiver path in the reference model (PREM [*Dziewonski and Anderson*, 1981]) and applied the weighting function. The weighted data are then summed to produce an estimate of velocity perturbation at the image point. In order to make the scattered wavefield a function of a single variable it is necessary to assume a proportionality between density and S-wave velocity anomalies ($\delta\ \rho/\rho = \kappa\delta\ \beta/\beta$). The constant of proportionality, κ, was taken as 0.3 [*Ranalli*, 1996]. To minimise errors associated with source positions and upper mantle structure all travel times and amplitudes are calculated relative to the direct *S* phase.

[8] The resolution of the migration results is tested by carrying out a series of forward calculations using the same source receiver geometries as the data. The forward calculations are also based upon single-scattering theory and ray theoretical Green's functions [*Chambers and Woodhouse*, 2006]. The synthetic scattered wavefield is calculated given a distribution and strength (S-wave velocity perturbation) for some scatterers. The response from large scattering bodies is approximated by using multiple point scatterers positioned at equally spaced points. The synthetic waveforms are then subjected to the to the same GRT analysis as the data.

3. Results

[9] Map views through the results from the weighted migration are shown in Figure 1 where the major feature is a positive velocity anomaly associated with the D″ discontinuity at approximately 2540 km depth. The discontinuity depth is slightly shallower than those reported by previous studies [e.g., *Gaherty and Lay*, 1992; *Houard and Nataf*, 1993; *Kendall and Shearer*, 1994; *Bilek and Lay*, 1998; *Thomas et al.*, 2002], which typically place the reflector in the depth range 2600–2580 km. However, given the spacing of the image points this discrepancy is not significant and can probably be attributed to the choice of reference model. There is also a smaller body in the southwest of the study area at 2740 km depth and complex structure near the base of the mantle at 2840 km depth.

[10] Figure 2a shows three example cross sections through the migration results. Near the centre of all three sections is the positive velocity anomaly associated with the D″ reflector in this region. The velocity contrasts retrieved by the GRT are of the order 1% for this reflector. However, the synthetic tests (Figures 2c and 2d) show that a velocity contrast of 3.0–3.5% in a thin layer is required to recreate the migration results.

[11] The North-South trending section in Figure 2 (A-A′) shows that the D″ reflector displays depth changes of around 100 km, and in sections B-B′ and C-C′ it can be seen that the reflector varies in amplitude across the section. At the position marked by the arrows in B-B′ the reflector stops, while in C-C′ it becomes less intense, indicating that the velocity contrast varies laterally. Comparison with Figure 2e shows that this occurs in well sampled region, and so should be well resolved. However, the results could still be biased by the source-receiver geometry and or reflector topography. To test this we perform synthetic tests in Figures 2c and 2d.

[12] In Figure 2c the D″ reflector is simulated using equally spaced point scatterers within a horizontal disc. In this case the reflector is equally visible along most of its length including the marked area where it is not seen in the data. The effect of discontinuity topography on the migra-

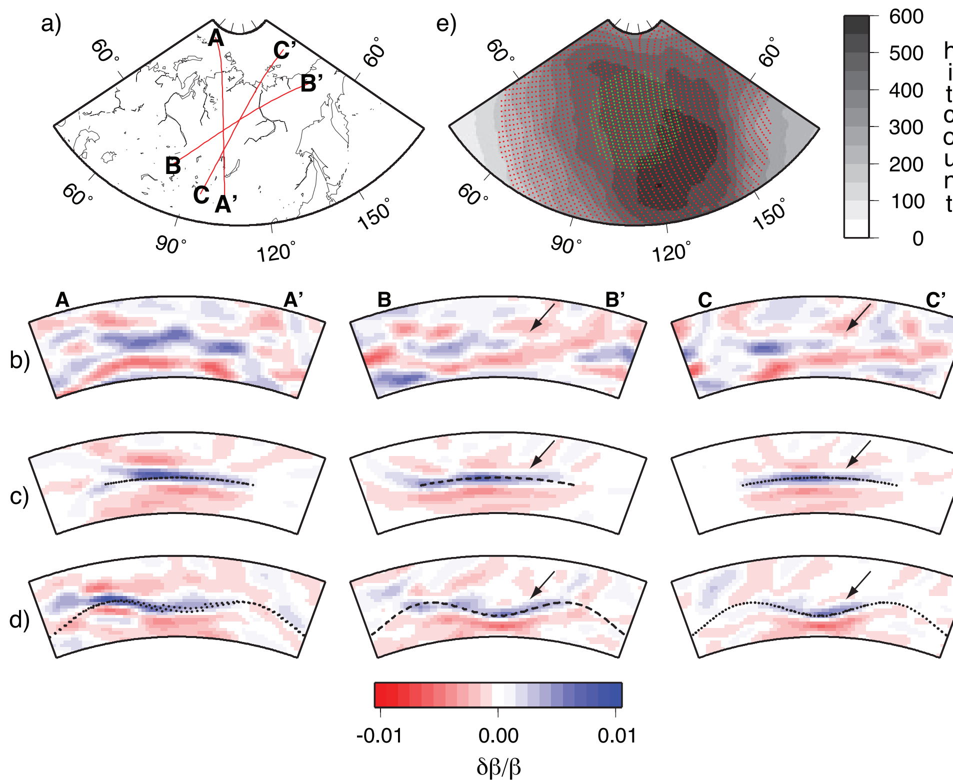

Figure 2. Cross-sections through (b) results of the weighted migration, and (c, d) synthetic tests. (a) Section orientations. Each section goes from 2090 km depth to the CMB, and is 40 in length. For the synthetic tests artificial data were generated using the forward model for the scattered wavefield [*Chambers and Woodhouse*, 2006]. Input models consist of discs with (Figure 2b) 800 km and (Figure 2c) 2250 km radius, made up of point scatterers spaced at 50 km intervals with S-wave velocity contrasts of 3.5 and 3.0% in Figures 2b and 2c respectively. For the larger disc (Figure 2c) 200 km peak to peak topography with a wavelength of 1500 km has been added. (e) Locations of the point scatterers in each model (red/green dots), as well as the hitcount at 2540 km depth (grayscale background). Hitcount is the number of time samples stacked at each image point. The black dots in the cross sections Figures 2b, 2c and 2d) mark the positions of point scatterers projected from 100 km either side of the section line. Arrows mark the position where the D″ reflector stops, in the northeast of the study region.

tion results is investigated in Figure 2d. The input model includes 200 km peak to peak depth variations, as indicated by previous observations of D″ topography [*Thomas et al.*, 2004b]. In this case the reflector extends over a wider area but it is not well retrieved near the edges of the sections. However, near the centre the reflector is still visible in the marked regions where it is absent from the data.

[13] In Figure 3 we compare the migration results with S-wave tomography model S20RTS [*Ritsema et al.*, 1999]. It can been seen in section A-A′ that the elevation in the D″ discontinuity corresponds to a region of high velocity. While in sections B-B′ and C-C′ the reflector is only present within this region of high velocity.

4. Discussion/Conclusion

[14] As the synthetic tests evaluate the response of scattering bodies by summing the contributions from point scatterers they include the effects of, uneven ray-path coverage, frequency dependence of the scattered waveforms, and uncertainties related to the Fresnel volumes. Factors such as the presence of lateral heterogeneity in the reference model are not accounted for, however, given the long-period nature of the data and measurement of the scattered wavefield relative to the direct S-wave, the influence of lateral heterogeneity on the migration results is minimal. Thus we believe that the results in Figure 2 show that the D″ reflector is resolvable in the marked regions, where it is absent from the data. This means that the D″ discontinuity is not a continuous surface, and the absence of the D″ discontinuity cannot be attributed to topography or focusing effects.

[15] A variation in the width of the discontinuity could create an apparent decrease in velocity contrast. Most estimates of the width of the D″ discontinuity are less than 50 km [*Wysession et al.*, 1998]. This is of the same order as the spacing for the migration grid, so variations in the discontinuity thickness will not be imaged with the current data set. Hence, we believe that the transient nature of the D″ discontinuity in this region is due to lateral variations in the velocity contrast along the reflector.

[16] The D″ discontinuity beneath North Central Asia appears to be restricted to a region of high seismic velocities (Figure 3). This high velocity feature in Figure 3 is sometimes associated with the subducted Izanagi plate [*Lithgow-Bertelloni and Richards*, 1998], which would

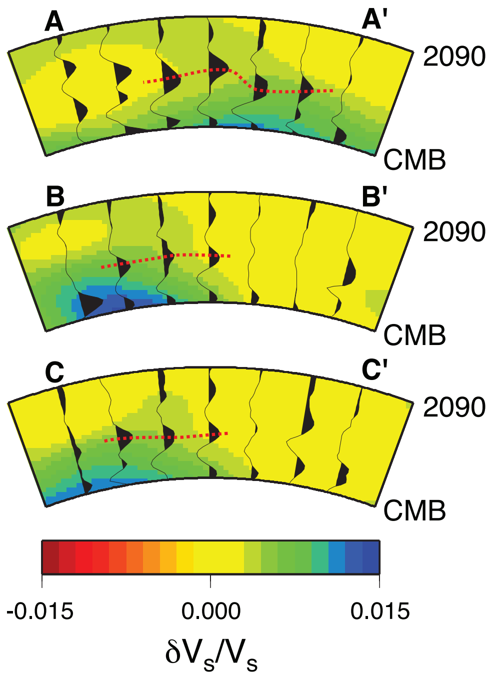

Figure 3. Comparison of depth profiles through the migration results (black traces) with seismic tomography model S20RTS (colour backgrounds [*Ritsema et al.*, 1999]). The location of the transects is given in Figure 2. The approximate position of the D″ reflector is marked by the red dashed line in each section.

suggest that the D″ reflector in this region is created by the associated changes in temperature, composition or phase.

[17] The results of this study are observations of lateral variation in the velocity contrast of the D″ discontinuity and areas where the reflector stops. The latter requires that lateral velocity gradients in the lower mantle are of the same order as the radial gradients, and places substantial constraints on the candidate explanations for the D″ discontinuity. Possible mechanisms for the D″ discontinuity include one or a combination of: steep thermal gradients, chemical heterogeneity and phase changes [*Wysession et al.*, 1998; *Lay and Garnero*, 2004; *Murakami et al.*, 2004]. If the discontinuity is caused by thermal or chemical effects then lateral heterogeneity could lead to a transient surface. However, *Wookey et al.* [2005] has shown that high frequency reflections are better explained by a phase transition of perovskite than by thermal gradients and, moreover, that the phase transition will be suppressed in high temperature regions. The cross-sections in Figure 3 could be interpreted in just this way, and so the termination may be confirmatory evidence of the existence and the behaviour of the post-perovskite phase transformation. It is also likely that compositional variations play a role.

[18] **Acknowledgments.** Seismic data were generated by the IRIS/IDA/USGS networks. K. C. was supported under the NERC studentship grant NER/S/A/2002/10529. This manuscript benefited from conversations with James Wookey and Mike Kendall as well as the contributions of two anonymous reviewers. The authors would also like to thank Ben Fox for improving the presentation of this manuscript. Data handling and computational infrastructure have been supported by NERC grants NER/F/S/2001/00369 and NE/B505997/1.

References

Bilek, S. L., and T. Lay (1998), Lower mantle heterogeneity beneath Eurasia imaged by parametric migration of shear waves, *Phys. Earth Planet. Inter.*, *108*, 201–218.

Castle, J. C., K. Creager, J. P. Winchester, and R. D. van der Hilst (2000), Shear wave speeds at the base of the mantle, *J. Geophys. Res.*, *105*, 21,543–21,557.

Chambers, K., and J. H. Woodhouse (2006), Investigating the lowermost mantle using migrations of long-period *S* – *ScS* data, *Geophys. J. Int.*, *106*, 667–678.

Dziewonski, A. M., and D. L. Anderson (1981), Preliminary Reference Earth Model, *Phys. Earth Planet. Inter.*, *25*, 297–356.

Gaherty, J. B., and T. Lay (1992), Investigation of laterally heterogeneous shear velocity structure in D″ beneath Eurasia, *J. Geophys. Res.*, *97*, 417–435.

Houard, S., and H. C. Nataf (1993), Laterally varying reflector at the top of the D″ beneath northern Siberia, *Geophys. J. Int.*, *115*, 168–182.

Hutko, A. R., T. Lay, E. J. Garnero, and J. Revenaugh (2006), Seismic detection of folded subducted lithosphere at the core-mantle boundary, *Nature*, *441*, 333–336.

Kendall, J. M., and P. M. Shearer (1994), Lateral variations in D″ thickness from long-period shear wave data, *J. Geophys. Res.*, *99*, 11,575–11,590.

Kito, T., and F. Kruger (2001), Heterogeneities in D″ beneath the southwestern Pacific inferred from scattered and reflected P-waves, *Geophys. Res. Lett.*, *28*, 2545–2548.

Lay, T., and E. J. Garnero (2004), Core-mantle boundary structures and processes, in *The State of the Planet: Frontiers and Challenges in Geophysics*, *Geophys. Monogr. Ser.*, vol. 150, edited by R. S. J. Sparks and C. J. Hawkesworth, pp. 25–42, AGU, Washington, D. C.

Lay, T., and D. V. Helmberger (1983), A lower mantle S-wave triplication and the shear velocity structure of D″, *Geophys. J. R. Astron. Soc.*, *75*, 799–838.

Lithgow-Bertelloni, C., and M. A. Richards (1998), The dynamics of Cenozoic and Mesozoic plate motions, *Rev. Geophys.*, *36*, 27–78.

Liu, X.-F., and A. M. Dziewonski (1998), Global analysis of shear wave velocity anomalies in the lower-most mantle, in *The Core-Mantle Boundary Region*, *Geodyn. Ser.*, vol. 28, edited by M. Gurnis et al., pp. 21–36, AGU, Washington, D. C.

Miller, D., M. Oristaglio, and G. Beylkin (1987), A new slant on seismic imaging: Migration and integral geometry, *Geophysics*, *52*, 943–964.

Murakami, M., K. Hirose, K. Kawamura, N. Sata, and Y. Ohishi (2004), Post-perovskite phase transition in $MgSiO_3$, *Science*, *304*, 855–857.

Ranalli, G. (1996), Seismic tomography and mineral physics, in *Seismic modelling of Earth structure*, pp. 443–461, Inst. Naz. de Geofis., Rome.

Ritsema, J., H. J. van Heijst, and J. H. Woodhouse (1999), Complex shear wave velocity structure imaged beneath Africa and Iceland, *Science*, *286*, 1925–1928.

Thomas, C., J. M. Kendall, and M. Weber (2002), The lowermost mantle beneath northern Asia: I. Multi-azimuth studies of a D″ heterogeneity, *Geophys. J. Int.*, *151*, 279–295.

Thomas, C., E. J. Garnero, and T. Lay (2004a), High resolution imaging of the lowermost mantle structure under the Cocos plate, *J. Geophys. Res.*, *109*, B08307, doi:10.1029/2004JB003013.

Thomas, C., J. M. Kendall, and J. Lowman (2004b), Lower-mantle seismic discontinuities and the thermal morphology of subducted slabs, *Earth Planet. Sci. Lett.*, *225*, 105–113.

Wookey, J., S. Stackhouse, J.-M. Kendall, J. Brodholt, and G. D. Price (2005), Efficacy of post-perovskite as an explanation for lowermost-mantle seismic properties, *Nature*, *438*, 1004–1007.

Wysession, M. E., T. Lay, J. Revenaugh, Q. Williams, E. J. Garnero, R. Jeanloz, and L. H. Kellogg (1998), The D″ discontinuity and its implications, in *The Core-Mantle Boundary Region*, *Geodyn. Ser.*, vol. 28, edited by M. Gurnis et al., pp. 273–297, AGU, Washington, D. C.

K. Chambers, Department of Earth Sciences, University of Bristol, Wills Memorial Building, Queen's Road, Bristol, BS8 1RJ, UK. (k.chambers@bristol.ac.uk)

J. H. Woodhouse, Department of Earth Sciences, University of Oxford, Parks road, Oxford, OX1 3PR, UK.